A Model for the Three-Level Cascade Atomic System

Matt Pennybacker

May 15, 2009

Abstract

With recent advances in optical materials, notably metamaterials, there is a need for more versatile models in nonlinear optics. Our goal is to develop a model for the one-dimensional propagation of electric fields in a resonant three-level medium. We develop a system of governing equations in a similar way to the well known two-level Maxwell-Bloch system. Once complete, we investigate possible computational methods that may be used to simulate the propagation of fields. Finally, we present computational results for special solutions of the two-level system along with steps for how these may be extended to three-level phenomena. Much of this work was done in collaboration with Dr. Ildar Gabitov and Dr. Shankar Venkataramani at The University of Arizona.

1 Introduction

The interaction of light and matter is a complicated process, but fortunately it can be simplified greatly while retaining a high degree of accuracy. The primary mechanism through which interaction occurs is polarization. For low-intensity pulses, much can be learned by approximating the polarization by a multiple of the electric field. In some circumstances, such as laser pulses, the intensity becomes high enough that the energy of the field is comparable to the intra-atom energy of the medium. This causes the approximation to break down and higher-order polarization terms to become important.

Although there are many ways to compensate for these effects, we hope to model the polarization from the point of view of quantum mechanics. Recall that a single atom has a large number of energy states. For simplicity, we will only consider three of these: a ground state and two excited states. This is referred to as the three-level cascade system, which is illustrated in Figure 1. Only transitions $|1\rangle \leftrightarrow |2\rangle$ and $|2\rangle \leftrightarrow |3\rangle$ are permitted. Respectively, these correspond to transition frequencies ω_{12} and ω_{23}. The three-level approximation is valid due to the fact that we are only considering fields near these frequencies.

2 Model

A mathematical model for the propagation of light in a resonant medium may be split into two coupled systems. The Bloch equations describe how the polarization of the medium evolves and the Maxwell equations describe how the electric field evolves. Together, they are known as the Maxwell-Bloch equations.

2.1 The Slowly Varying Envelope Approximation

We begin by describing the fields that will be modeled. It is reasonable to expect that the dominant interaction will be parallel, so we retain only scalar quantities and replace the inner product with multiplication.

Figure 1: Energy state diagram for the three-level cascade system.

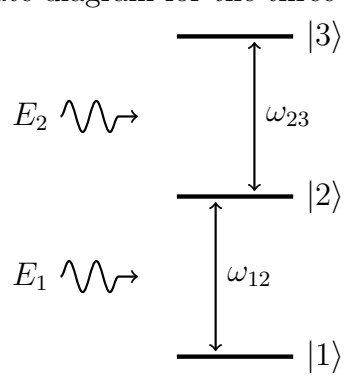

The electric field E may be written in terms of two near-resonant fields E_1 and E_2 with frequencies $\omega_1 \approx \omega_{12}$ and $\omega_2 \approx \omega_{23}$ respectively. We may, in turn, write E_1 and E_2 in terms of slowly varying envelopes as

$$E_1 = A_1^{(+)} e^{-i\omega_1 t + ik_1 z} + A_1^{(-)} e^{-i\omega_1 t - ik_1 z} + (*),$$
$$E_2 = A_2^{(+)} e^{-i\omega_2 t + ik_2 z} + A_2^{(-)} e^{-i\omega_2 t - ik_2 z} + (*).$$

Here, both fields are in a right-handed medium. Envelopes $A_1^{(+)}$ and $A_2^{(+)}$ correspond to forward propagating fields; envelopes $A_1^{(-)}$ and $A_2^{(-)}$ correspond to backward propagating fields. Assuming their bandwidths are narrow, we may substitute these expressions for E_1 and E_2 and neglect any rapidly varying components of the solution.

2.2 The Maxwell Equations

We will return to the slowly varying envelope approximation following a short discussion of the vector fields $\vec{E}$, $\vec{D}$, $\vec{B}$, and $\vec{H}$. These are the electric field, electric displacement field, magnetic field, and magnetizing field respectively. In a dielectric medium with no free charges and in which no current flows, the Maxwell equations are

$$\nabla \cdot \vec{D} = 0, \tag{1}$$
$$\nabla \cdot \vec{B} = 0, \tag{2}$$
$$\nabla \times \vec{E} = -\frac{\partial \vec{B}}{\partial t}, \tag{3}$$
$$\nabla \times \vec{H} = \frac{\partial \vec{D}}{\partial t}. \tag{4}$$

Coupled with these are the constitutive relations $\vec{D} = \epsilon \vec{E} = \epsilon_0 \vec{E} + \vec{P}$ and $\vec{B} = \mu_0 \vec{H}$.

Our goal is to describe the general relationship between the electric field $\vec{E}$ and polarization $\vec{P}$. Taking the curl of (3) yields

$$\nabla^2 \vec{E} - \nabla(\nabla \cdot \vec{E}) = -\nabla \times \frac{\partial \vec{B}}{\partial t}.$$

We may then substitute (4) to find

$$\nabla^2 \vec{E} - \nabla(\nabla \cdot \vec{E}) = -\mu_0 \frac{\partial^2 \vec{D}}{\partial t^2}.$$

Thus, the single governing equation is given by

$$\nabla^2 \vec{E} - \frac{1}{c^2}\frac{\partial^2 \vec{E}}{\partial t^2} - \nabla(\nabla \cdot \vec{E}) = \frac{1}{\epsilon_0 c^2}\frac{\partial^2 \vec{P}}{\partial t^2}. \tag{5}$$

Furthermore, we may assume that $\vec{P}$ varies slowly over a single wavelength and so (1) implies that $\nabla \cdot \vec{E} \approx 0$. Taking $\vec{E}$ and $\vec{P}$ parallel reduces (5) to the familiar wave equation

$$\frac{\partial^2 E}{\partial z^2} - \frac{1}{c^2}\frac{\partial^2 E}{\partial t^2} = \frac{1}{\epsilon_0 c^2}\frac{\partial^2 P}{\partial t^2}. \tag{6}$$

We now hope to take advantage of the assumptions made in the slowly varying envelope approximation. The Fourier transform of (6) is

$$\left(k^2 - \frac{\omega^2}{c^2}\right)\hat{E} = \frac{\omega^2}{\epsilon_0 c^2}\hat{P}.$$

Next, separating the polarization into a linear term $\hat{P}_e = \chi_e \hat{E}$ and a nonlinear resonant term $\hat{P}_r$ yields

$$\left(k^2 - \frac{\omega^2}{c^2}\epsilon_r\right)\hat{E} = \frac{\omega^2}{\epsilon_0 c^2}\hat{P}_r,$$

where $\epsilon_r = 1 + \chi_e$ is the relative permittivity. The remaining calculations are similar for each of the envelopes, so we will focus on the slowly varying envelope $A_1^{(+)}$. Let $\Lambda_1^{(+)}$ be the corresponding slowly varying envelope for the resonant polarization. If we write $\omega = \omega_1 + \Delta\omega$ and $k = k_1 + \Delta k$, it is necessary to consider only $\Delta\omega \ll \omega_1$ and $\Delta k \ll k_1$ in the approximation. Doing this, we find that

$$\left((k_1 + \Delta k)^2 - \frac{(\omega_1 + \Delta\omega)^2}{c^2}\epsilon_r(\omega_1 + \Delta\omega)\right)\hat{A}_1^{(+)} = \frac{(\omega_1 + \Delta\omega)^2}{\epsilon_0 c^2}\hat{\Lambda}_1^{(+)}.$$

Terms that are second-order or higher in $\Delta\omega$ and Δk may be neglected. Thus, expanding ϵ_r in a series about ω_1 yields

$$\left(2k_1\Delta k - \frac{\omega_1^2}{c^2}\epsilon_r'(\omega_1)\Delta\omega - \frac{2\omega_1}{c^2}\epsilon_r(\omega_1)\Delta\omega\right)\hat{A}_1^{(+)} = \frac{\omega_1^2}{\epsilon_0 c^2}\hat{\Lambda}_1^{(+)}.$$

This may be further simplified by observing that

$$\frac{\omega_1^2}{c^2}\epsilon_r'(\omega_1) + \frac{2\omega_1}{c^2}\epsilon_r(\omega_1) = \frac{d}{d\omega}\left(\frac{\omega^2}{c^2}\epsilon_r(\omega)\right)\bigg|_{\omega=\omega_1} = \frac{d}{d\omega}k^2\bigg|_{k=k_1} = 2\frac{k_1}{v_1},$$

where v_1 is the group velocity. Making this substitution yields

$$\left(\Delta k - \frac{1}{v_1}\Delta\omega\right)\hat{A}_1^{(+)} = \frac{\omega_1^2}{2k_1\epsilon_0 c^2}\hat{\Lambda}_1^{(+)},$$

which has the inverse Fourier transform

$$\left(\frac{\partial}{\partial z} + \frac{1}{v_1}\frac{\partial}{\partial t}\right)A_1^{(+)} = \frac{i\omega_1^2}{2k_1\epsilon_0 c^2}\Lambda_1^{(+)}. \tag{7}$$

This is the customary form of the governing equation for a slowly varying envelope. The remaining equations are given by

$$\left(\frac{\partial}{\partial z} - \frac{1}{v_1}\frac{\partial}{\partial t}\right) A_1^{(-)} = \frac{i\omega_1^2}{2k_1\epsilon_0 c^2}\Lambda_1^{(-)}, \tag{8}$$

$$\left(\frac{\partial}{\partial z} + \frac{1}{v_2}\frac{\partial}{\partial t}\right) A_2^{(+)} = \frac{i\omega_2^2}{2k_2\epsilon_0 c^2}\Lambda_2^{(+)}, \tag{9}$$

$$\left(\frac{\partial}{\partial z} - \frac{1}{v_2}\frac{\partial}{\partial t}\right) A_2^{(-)} = \frac{i\omega_2^2}{2k_2\epsilon_0 c^2}\Lambda_2^{(-)}. \tag{10}$$

2.3 The Bloch Equations

In its unperturbed ground state, the electron cloud of an atom is spherically symmetric about the nucleus. This cloud will be distorted under the influence of an electric field. An oscillating dipole oriented in the direction of the field will be created which will, in turn, radiate its own electric field. The net effect of many such atoms is described by the resonant polarization density P_r. Writing this in terms of slowly varying envelopes gives $\Lambda_1^{(+)}$, $\Lambda_1^{(-)}$, $\Lambda_2^{(+)}$, and $\Lambda_2^{(-)}$ from the field equations.

The density matrix $\hat{\rho}$ associated with an atom is the statistical description of its mixed quantum state. In general, it may be given by

$$\hat{\rho} = \begin{bmatrix} \rho_{11} & \rho_{12} & \rho_{13} \\ \rho_{12}^* & \rho_{22} & \rho_{23} \\ \rho_{13}^* & \rho_{23}^* & \rho_{33} \end{bmatrix}$$

for a system with three eigenstates. Diagonal entries are the populations of each energy level, with $\rho_{11} + \rho_{22} + \rho_{33} = 1$. It is well known that the expectation value of any observable $\hat{A}$ is given by

$$\langle \hat{A} \rangle = \mathrm{Tr}(\hat{\rho}\hat{A}). \tag{11}$$

We are particularly interested in the dipole matrix $\hat{d}$, since the resonant polarization density of a single atom is given by its expectation value. Thus, the evolution of the density matrix contains all the information necessary to construct the resonant polarization.

The Hamiltonian $\hat{H}$ for this system may be written in terms of an unperturbed matrix $\hat{H}_0$ and an atom-field interaction matrix $\hat{H}_{A-F}$. The unperturbed Hamiltonian describes the three equilibrium energy levels. Normalizing the energy of the ground state to zero, we find that

$$\hat{H}_0 = \begin{bmatrix} 0 & 0 & 0 \\ 0 & \hbar\omega_{12} & 0 \\ 0 & 0 & \hbar\omega_{13} \end{bmatrix}.$$

There are two assumptions that are important in simplifying the atom-field interaction. First, the atoms interact with the field roughly as classical electric dipoles. This is valid whenever the atomic length scale is much smaller than the wavelength of the electric field.

Second, we assume that each transition dipole element interacts only with the electric field corresponding to its transition. The general dipole matrix may be given by

$$\hat{d} = \begin{bmatrix} 0 & d_{12} & d_{13} \\ d_{12}^* & 0 & d_{23} \\ d_{13}^* & d_{23}^* & 0 \end{bmatrix},$$

where the zero diagonal entries are due to the lack of a permanent dipole moment. The atom-field interaction Hamiltonian is then given by the energy $-\hat{d}E$ of the induced dipole in the electric field. All together, this implies that

$$\hat{H}_{A-F} = \begin{bmatrix} 0 & -d_{12}E_1 & 0 \\ -d_{12}^*E_1 & 0 & -d_{23}E_2 \\ 0 & -d_{23}^*E_2 & 0 \end{bmatrix}.$$

The complete Hamiltonian is given by $\hat{H} = \hat{H}_0 + \hat{H}_{A-F}$. Now, recall that the Von Neumann equation states

$$\frac{\partial \hat{\rho}}{\partial t} = \frac{i}{\hbar}[\hat{H}, \hat{\rho}]. \tag{12}$$

The trace of $\hat{\rho}$ is conserved in this expression, so there are only two independent quantities relating the diagonal entries of $\hat{\rho}$. Writing these as $n_1 = \rho_{22} - \rho_{11}$ and $n_2 = \rho_{22} - \rho_{33}$, expansion of (12) yields

$$\frac{\partial n_1}{\partial t} = \frac{2i}{\hbar}(d_{12}E_1\rho_{12}^* - d_{12}^*E_1\rho_{12}) - \frac{i}{\hbar}(d_{23}E_2\rho_{23}^* - d_{23}^*E_2\rho_{23}), \tag{13}$$

$$\frac{\partial n_2}{\partial t} = \frac{2i}{\hbar}(d_{23}E_2\rho_{23}^* - d_{23}^*E_2\rho_{23}) - \frac{i}{\hbar}(d_{12}E_1\rho_{12}^* - d_{12}^*E_1\rho_{12}), \tag{14}$$

$$\frac{\partial \rho_{12}}{\partial t} = -i\omega_{12}\rho_{12} - \frac{i}{\hbar}d_{12}E_1n_1 + \frac{i}{\hbar}d_{23}^*E_2\rho_{13}, \tag{15}$$

$$\frac{\partial \rho_{23}}{\partial t} = -i\omega_{23}\rho_{23} + \frac{i}{\hbar}d_{23}E_2n_2 - \frac{i}{\hbar}d_{12}^*E_1\rho_{13}, \tag{16}$$

$$\frac{\partial \rho_{13}}{\partial t} = -i\omega_{13}\rho_{13} - \frac{i}{h}d_{12}E_1\rho_{23} + \frac{i}{h}d_{23}E_2\rho_{12}. \tag{17}$$

The next step is to express (15)-(17) in terms of slowly varying envelopes. We expect that ρ_{12} and ρ_{23} will oscillate with frequencies ω_1 and ω_2 respectively. Thus, we write

$$\rho_{12} = \sigma_{12}^{(+)}e^{-i\omega_1 t + ik_1 z} + \sigma_{12}^{(-)}e^{-i\omega_1 t - ik_1 z},$$
$$\rho_{23} = \sigma_{23}^{(+)}e^{-i\omega_2 t + ik_2 z} + \sigma_{23}^{(-)}e^{-i\omega_2 t - ik_2 z}.$$

The entry ρ_{13} requires a touch of care. It is here, roughly, that any interaction between the two electric fields takes place. The frequency of any oscillation generated in this entry is $\omega_1 + \omega_2$. The associated wavenumber depends on the relative directions of propagation. Specifically, co-propagating fields corresponds to wavenumbers $k_1 + k_2$ and $-(k_1 + k_2)$.

Counter-propagating fields correspond to wavenumbers $k_1 - k_2$ and $-(k_1 - k_2)$. Hence,

$$\rho_{13} = \sigma_{13}^{(+,+)} e^{-i(\omega_1+\omega_2)t+i(k_1+k_2)z} + \sigma_{13}^{(-,-)} e^{-i(\omega_1+\omega_2)t-i(k_1+k_2)z} + \sigma_{13}^{(+,-)} e^{-i(\omega_1+\omega_2)t+i(k_1-k_2)z} + \sigma_{13}^{(-,+)} e^{-i(\omega_1+\omega_2)t-i(k_1-k_2)z}.$$

Substituting the slowly varying envelopes into (13)-(17) and collecting terms yields

$$\frac{\partial n_1}{\partial t} = \frac{2i}{\hbar}(d_{12}A_1^{(+)}\sigma_{12}^{(+)*} + d_{12}A_1^{(-)}\sigma_{12}^{(-)*} - d_{12}^*A_1^{(+)*}\sigma_{12}^{(+)} - d_{12}^*A_1^{(-)*}\sigma_{12}^{(-)}) - \frac{i}{\hbar}(d_{23}A_2^{(+)}\sigma_{23}^{(+)*} + d_{23}A_2^{(-)}\sigma_{23}^{(-)*} - d_{23}^*A_2^{(+)*}\sigma_{23}^{(+)} - d_{23}^*A_2^{(-)*}\sigma_{23}^{(-)}), \tag{18}$$

$$\frac{\partial n_2}{\partial t} = \frac{2i}{\hbar}(d_{23}A_2^{(+)}\sigma_{23}^{(+)*} + d_{23}A_2^{(-)}\sigma_{23}^{(-)*} - d_{23}^*A_2^{(+)*}\sigma_{23}^{(+)} - d_{23}^*A_2^{(-)*}\sigma_{23}^{(-)}) - \frac{i}{\hbar}(d_{12}A_1^{(+)}\sigma_{12}^{(+)*} + d_{12}A_1^{(-)}\sigma_{12}^{(-)*} - d_{12}^*A_1^{(+)*}\sigma_{12}^{(+)} - d_{12}^*A_1^{(-)*}\sigma_{12}^{(-)}), \tag{19}$$

$$\frac{\partial \sigma_{12}^{(+)}}{\partial t} = i(\omega_1 - \omega_{12})\sigma_{12}^{(+)} - \frac{i}{\hbar}d_{12}A_1^{(+)}n_1 + \frac{i}{\hbar}(d_{23}^*A_2^{(+)*}\sigma_{13}^{(+,+)} + d_{23}^*A_2^{(-)*}\sigma_{13}^{(+,-)}), \tag{20}$$

$$\frac{\partial \sigma_{12}^{(-)}}{\partial t} = i(\omega_1 - \omega_{12})\sigma_{12}^{(-)} - \frac{i}{\hbar}d_{12}A_1^{(-)}n_1 + \frac{i}{\hbar}(d_{23}^*A_2^{(+)*}\sigma_{13}^{(-,+)} + d_{23}^*A_2^{(-)*}\sigma_{13}^{(-,-)}), \tag{21}$$

$$\frac{\partial \sigma_{23}^{(+)}}{\partial t} = i(\omega_2 - \omega_{23})\sigma_{23}^{(+)} + \frac{i}{\hbar}d_{23}A_2^{(+)}n_2 - \frac{i}{\hbar}(d_{12}^*A_1^{(+)*}\sigma_{13}^{(+,+)} + d_{12}^*A_1^{(-)*}\sigma_{13}^{(-,+)}), \tag{22}$$

$$\frac{\partial \sigma_{23}^{(-)}}{\partial t} = i(\omega_2 - \omega_{23})\sigma_{23}^{(-)} + \frac{i}{\hbar}d_{23}A_2^{(-)}n_2 - \frac{i}{\hbar}(d_{12}^*A_1^{(+)*}\sigma_{13}^{(+,-)} + d_{12}^*A_1^{(-)*}\sigma_{13}^{(-,-)}), \tag{23}$$

$$\frac{\partial \sigma_{13}^{(+,+)}}{\partial t} = i(\omega_1 + \omega_2 - \omega_{13})\sigma_{13}^{(+,+)} - \frac{i}{\hbar}d_{12}A_1^{(+)}\sigma_{23}^{(+)} + \frac{i}{\hbar}d_{23}A_2^{(+)}\sigma_{12}^{(+)}, \tag{24}$$

$$\frac{\partial \sigma_{13}^{(-,-)}}{\partial t} = i(\omega_1 + \omega_2 - \omega_{13})\sigma_{13}^{(-,-)} - \frac{i}{\hbar}d_{12}A_1^{(-)}\sigma_{23}^{(-)} + \frac{i}{\hbar}d_{23}A_2^{(-)}\sigma_{12}^{(-)}, \tag{25}$$

$$\frac{\partial \sigma_{13}^{(+,-)}}{\partial t} = i(\omega_1 + \omega_2 - \omega_{13})\sigma_{13}^{(+,-)} - \frac{i}{\hbar}d_{12}A_1^{(+)}\sigma_{23}^{(-)} + \frac{i}{\hbar}d_{23}A_2^{(-)}\sigma_{12}^{(+)}, \tag{26}$$

$$\frac{\partial \sigma_{13}^{(-,+)}}{\partial t} = i(\omega_1 + \omega_2 - \omega_{13})\sigma_{13}^{(-,+)} - \frac{i}{\hbar}d_{12}A_1^{(-)}\sigma_{23}^{(+)} + \frac{i}{\hbar}d_{23}A_2^{(+)}\sigma_{12}^{(-)}. \tag{27}$$

Finally, we must find the resonant polarization in terms of density matrix entries. This quantity is given for a single atom by the expected value of the dipole matrix

$$\langle \hat{d} \rangle = \mathrm{Tr}(\hat{\rho}\,\hat{d}) = d_{12}\rho_{12}^* + d_{12}^*\rho_{12} + d_{23}\rho_{23}^* + d_{23}^*\rho_{23} + d_{13}\rho_{13}^* + d_{13}^*\rho_{13}.$$

If there are n_a atoms interacting with the field, substituting the slowly varying envelopes into this expression as and collecting terms yields

$$\Lambda_1^{(+)} = n_a d_{12}^* \sigma_{12}^{(+)}, \qquad \Lambda_1^{(-)} = n_a d_{12}^* \sigma_{12}^{(-)},$$
$$\Lambda_2^{(+)} = n_a d_{23}^* \sigma_{23}^{(+)}, \qquad \Lambda_2^{(-)} = n_a d_{23}^* \sigma_{23}^{(-)}.$$

2.4 Nondimensionalization

Let t_c and z_c be the characteristic time scale and length scale respectively. The corresponding nondimensional variables are

$$\bar{t} = \frac{t}{t_c}, \qquad \bar{z} = \frac{z}{z_c}.$$

In order to eliminate all dimensional parameters in (7) and (8), we choose characteristic scales

$$t_c = \sqrt{\frac{2\hbar k_1 \epsilon_0 c^2}{v_1 n_a \omega_1^2 |d_{12}|^2}}, \qquad z_c = \sqrt{\frac{2 v_1 \hbar k_1 \epsilon_0 c^2}{n_a \omega_1^2 |d_{12}|^2}}.$$

Note that the induced characteristic velocity is z_c/t_c is v_1. The Rabi frequency associated with a transition is a measure of the coupling between the field and the polarization. For example, the frequency associated with the field $A_1^{(+)}$ is $d_{12}A_1^{(+)}/\hbar$. It is convenient to exploit this by choosing rescaled field envelopes

$$\bar{A}_1^{(+)} = \frac{t_c d_{12}}{\hbar} A_1^{(+)}, \qquad \bar{A}_1^{(-)} = \frac{t_c d_{12}}{\hbar} A_1^{(-)},$$
$$\bar{A}_2^{(+)} = \frac{t_c d_{23}}{\hbar} A_2^{(+)}, \qquad \bar{A}_2^{(-)} = \frac{t_c d_{23}}{\hbar} A_2^{(-)}.$$

The nondimensional parameters that remain after making these substitutions are

$$\delta_1 = t_c(\omega_1 - \omega_{12}), \qquad \delta_2 = t_c(\omega_2 - \omega_{23}),$$
$$\nu = \frac{v_1}{v_2}, \qquad \eta = \frac{\omega_1^2 k_2 |d_{12}|^2}{\omega_2^2 k_1 |d_{23}|^2}.$$

Parameters δ_1 and δ_2 indicate the amount of detuning, which causes the phase of the polarization to rotate continuously. Both are zero if we only consider perfect resonance. Parameters ν and η indicate how the medium responds to the two transition frequencies. Now, the

model is given by

$$\left(\frac{\partial}{\partial \bar{z}} + \frac{\partial}{\partial \bar{t}}\right) \bar{A}_1^{(+)} = \sigma_{12}^{(+)}, \tag{28}$$

$$\left(\frac{\partial}{\partial \bar{z}} - \frac{\partial}{\partial \bar{t}}\right) \bar{A}_1^{(-)} = \sigma_{12}^{(-)}, \tag{29}$$

$$\left(\frac{\partial}{\partial \bar{z}} + \nu\frac{\partial}{\partial \bar{t}}\right) \bar{A}_2^{(+)} = \eta\sigma_{23}^{(+)}, \tag{30}$$

$$\left(\frac{\partial}{\partial \bar{z}} - \nu\frac{\partial}{\partial \bar{t}}\right) \bar{A}_2^{(-)} = \eta\sigma_{23}^{(-)}, \tag{31}$$

$$\begin{aligned}\frac{\partial n_1}{\partial \bar{t}} &= 2i(\bar{A}_1^{(+)}\sigma_{12}^{(+)*} + \bar{A}_1^{(-)}\sigma_{12}^{(-)*} - \bar{A}_1^{(+)*}\sigma_{12}^{(+)} - \bar{A}_1^{(-)*}\sigma_{12}^{(-)}) \\ &\quad - i(\bar{A}_2^{(+)}\sigma_{23}^{(+)*} + \bar{A}_2^{(-)}\sigma_{23}^{(-)*} - \bar{A}_2^{(+)*}\sigma_{23}^{(+)} - \bar{A}_2^{(-)*}\sigma_{23}^{(-)}),\end{aligned} \tag{32}$$

$$\begin{aligned}\frac{\partial n_2}{\partial \bar{t}} &= 2i(\bar{A}_2^{(+)}\sigma_{23}^{(+)*} + \bar{A}_2^{(-)}\sigma_{23}^{(-)*} - \bar{A}_2^{(+)*}\sigma_{23}^{(+)} - \bar{A}_2^{(-)*}\sigma_{23}^{(-)}) \\ &\quad - i(\bar{A}_1^{(+)}\sigma_{12}^{(+)*} + \bar{A}_1^{(-)}\sigma_{12}^{(-)*} - \bar{A}_1^{(+)*}\sigma_{12}^{(+)} - \bar{A}_1^{(-)*}\sigma_{12}^{(-)}),\end{aligned} \tag{33}$$

$$\frac{\partial \sigma_{12}^{(+)}}{\partial \bar{t}} = i\delta_1\sigma_{12}^{(+)} - i\bar{A}_1^{(+)}n_1 + i\bar{A}_2^{(+)*}\sigma_{13}^{(+,+)} + i\bar{A}_2^{(-)*}\sigma_{13}^{(+,-)}, \tag{34}$$

$$\frac{\partial \sigma_{12}^{(-)}}{\partial \bar{t}} = i\delta_1\sigma_{12}^{(-)} - i\bar{A}_1^{(-)}n_1 + i\bar{A}_2^{(+)*}\sigma_{13}^{(-,+)} + i\bar{A}_2^{(-)*}\sigma_{13}^{(-,-)}, \tag{35}$$

$$\frac{\partial \sigma_{23}^{(+)}}{\partial \bar{t}} = i\delta_2\sigma_{23}^{(+)} + i\bar{A}_2^{(+)}n_2 - i\bar{A}_1^{(+)*}\sigma_{13}^{(+,+)} - i\bar{A}_1^{(-)*}\sigma_{13}^{(-,+)}, \tag{36}$$

$$\frac{\partial \sigma_{23}^{(-)}}{\partial \bar{t}} = i\delta_2\sigma_{23}^{(-)} + i\bar{A}_2^{(-)}n_2 - i\bar{A}_1^{(+)*}\sigma_{13}^{(+,-)} - iA_1^{(-)*}\sigma_{13}^{(-,-)}, \tag{37}$$

$$\frac{\partial \sigma_{13}^{(+,+)}}{\partial \bar{t}} = i(\delta_1 + \delta_2)\sigma_{13}^{(+,+)} - i\bar{A}_1^{(+)}\sigma_{23}^{(+)} + i\bar{A}_2^{(+)}\sigma_{12}^{(+)}, \tag{38}$$

$$\frac{\partial \sigma_{13}^{(-,-)}}{\partial \bar{t}} = i(\delta_1 + \delta_2)\sigma_{13}^{(-,-)} - i\bar{A}_1^{(-)}\sigma_{23}^{(-)} + i\bar{A}_2^{(-)}\sigma_{12}^{(-)}, \tag{39}$$

$$\frac{\partial \sigma_{13}^{(+,-)}}{\partial \bar{t}} = i(\delta_1 + \delta_2)\sigma_{13}^{(+,-)} - i\bar{A}_1^{(+)}\sigma_{23}^{(-)} + i\bar{A}_2^{(-)}\sigma_{12}^{(+)}, \tag{40}$$

$$\frac{\partial \sigma_{13}^{(-,+)}}{\partial \bar{t}} = i(\delta_1 + \delta_2)\sigma_{13}^{(-,+)} - i\bar{A}_1^{(-)}\sigma_{23}^{(+)} + i\bar{A}_2^{(+)}\sigma_{12}^{(-)}. \tag{41}$$

This agrees with the model for co-propagating fields described in both [3] and [2], but it also includes equations describing counter-propagating fields.

3 Computation

The next step is to develop a computational method for integrating (28)-(41). A naïve attempt can be made using finite differences, but there are much more effective methods which take advantage of the structure of this system of equations. This is a description of one such method.

3.1 Initial Observations

Figure 2: Stencil for the proposed numerical method with equal group velocities.

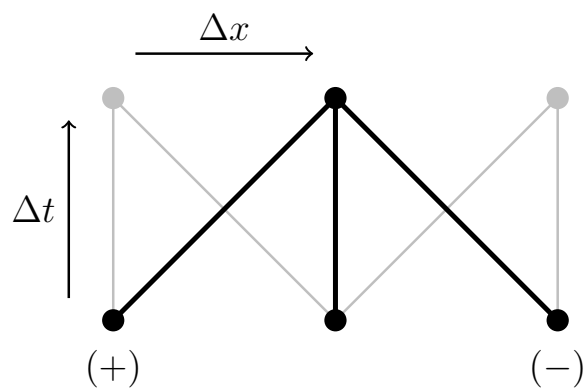

Figure 3: Stencil for the proposed numerical method with unequal group velocities.

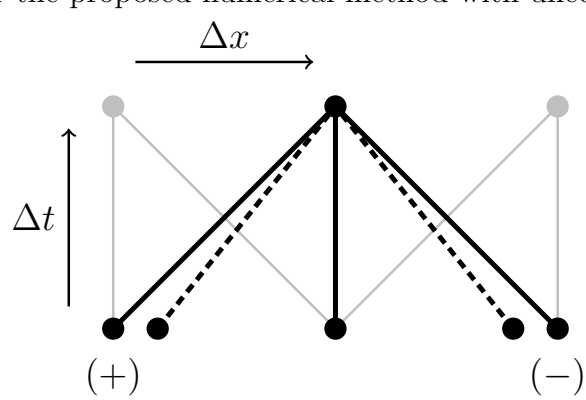

We first consider the case in which the electric fields have equal group velocities. In other words, let $\nu = 1$. The only space derivatives occur in the inhomogeneous advection-type field equations (28)-(31). Characteristics for these are lines with unit slope in the phase space. The material variables propagate along vertical characteristics. We may exploit this by choosing a mesh with $\Delta x = \Delta t$ as in Figure 2. Here, forward propagating fields begin at the point marked $(+)$ and backward propagating fields begin at the point marked $(-)$. Characteristics ending at adjacent mesh points are marked in gray.

It is clear that counter-propagating fields interact between mesh points. Hence, it is desirable to choose a method that only uses data from mesh points to avoid interpolation. The highest-order convergence in this case is given by the trapezoid method. One possible drawback is that this method is implicit, but this can be resolved using iteration.

Next, we consider the case in which the electric fields have different group velocities. It makes sense to align the mesh with one of these. The remaining field may be addressed through interpolation in two ways. First, it is possible to ensure that all field variables end on a mesh point and interpolate where they begin as illustrated in Figure 3. Dotted lines represent the true characteristics of the fields interpolated between mesh points. This has the advantage of interpolating explicit data, but it is necessary to interpolate the material variables in addition to the field variables. Alternatively, it is possible to ensure that all field variables begin on a mesh point and interpolate where they end as illustrated in Figure 4. This has the disadvantage of interpolating implicit data, which is relatively expensive to implement. Thus, only the former interpolation scheme is considered though the latter may yield comparable results.

3.2 Implementation

We have chosen to implement this as an initial boundary value problem in MATLAB for simplicity, but it may be easily modified for any language with a full-featured matrix algebra library. The boundary conditions specify the electric field propagating into the domain and are given as an arbitrary routine. In addition, an initial condition and a routine to evaluate (28)-(41) at each mesh point must be given.

We hope to use an iteration scheme as stated earlier to make the trapezoid method explicit. The most common scheme used for this purpose is Newton iteration, but it relies on the calculation of the Jacobian matrix. The presence of conjugation in the system of equations makes this particularly difficult. On the other hand, it is not clear that fixed-point iteration necessarily converges. In practice, though, the fixed-point scheme is effective.

Figure 4: Alternative stencil for the proposed numerical method with unequal group velocities.

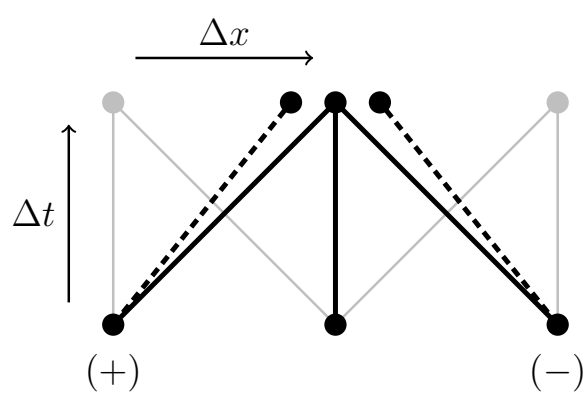

The error may be estimated from the difference of two consecutive iterations. Pseudocode for the trapezoid method implemented this way follows in Algorithm 1.

Algorithm 1 Iterative Trapezoid Method on Characteristics

```
evaluate the initial system of equations
shift variables along characteristics (interpolate if necessary)
evaluate the boundary conditions
calculate a prediction for the final value using the Euler method
repeat
    evaluate the final system of equations
    calculate a prediction for the final value using the trapezoid method
until error is within tolerance
```

The only remaining detail is the interpolation method that will be used if the group velocities are different. Linear interpolation is inexpensive, but it results in significant numerical dispersion at moderate differences in velocity. Cubic spline interpolation and piecewise cubic hermite polynomial (PCHIP) interpolation both reduce numerical artifacts but are significantly more expensive. In fact, they consume approximately two-thirds of the computation time when enabled. The optimal choice requires more investigation, but the current implementation uses cubic splines.

3.3 Verification

Once the integration routine has been written, it is necessary to verify that it behaves as expected. The simplest test is for second-order convergence. Step doubling is a technique in which the step size is reduced by a factor of two and the solutions are compared at the common mesh points. The rate of convergence may be estimated in this way. Indeed, it indicates that convergence occurs as expected.

We may also observe that the density matrix satisfies a Liouville equation. This implies that $\mathrm{Tr}(\hat{\rho})$, $\mathrm{Tr}(\hat{\rho}^2)$, and $\mathrm{Tr}(\hat{\rho}^3)$ are conserved quantities. These may be computed inexpensively and monitored during integration. More generally, the eigenvalues of the density matrix are conserved. Truncation error and roundoff error both contribute to changes these quantities, but the deviation of the eigenvalues is less than 0.01% in all test cases.

4 Results

Finally, there are a number of results for the two-level system that can be integrated using this computational method. These not only serve as good test cases, but they are also related to results in the three-level system that have yet to be explored analytically. Presented here are the computational results along with next steps for future research.

4.1 Optical Solitons

A soliton is a solitary wave that propagates unchanged through a nonlinear medium. This occurs due to a balance between nonlinear effects and linear effects such as diffraction and dispersion. In optics, this phenomenon is known at self-induced transparency. Specific solutions may be found using the inverse scattering technique as in [3] or by a co-moving coordinate transformation as in [1]. We use the results from the latter, although the former is significantly more versatile.

The equation for a simple forward propagating soliton is given by

$$A_1^{(+)}(\zeta) = \frac{1}{\kappa\tau} \operatorname{sech}\left(\frac{\zeta}{\tau}\right).$$

Here, $\zeta = z - t/V$ is the co-moving coordinate with velocity V. The parameter κ depends on the scaling of the electric field amplitude, and the free parameter τ determines the amplitude of the pulse. The velocity depends on the amplitude of the soliton; more intense pulses travel faster.

Figure 5: Single optical soliton with $\kappa = 1$, $\tau = 0.5$.

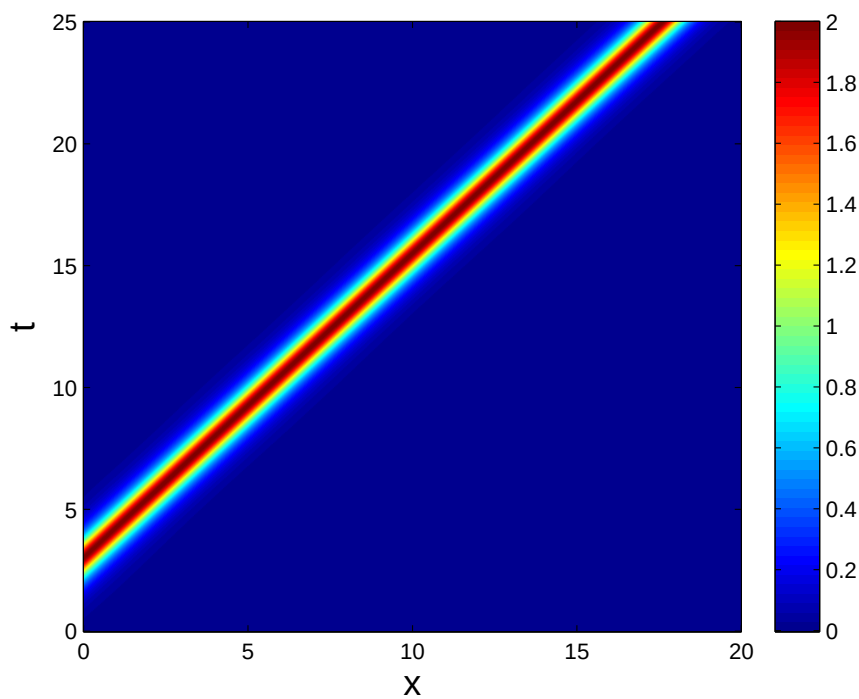

The propagation of a single soliton is illustrated in Figure 5. At any point in time, the profile of the field can be found by taking a horizontal slice. Note that the pulse indeed travels slower than the group velocity; this is due to the interaction of the field and the medium. A large portion of the energy in the pulse is transferred to the medium through single photon

absorption. The medium then transfers energy back to the field through emission. This makes it a good test scenario for the computational method.

Figure 6: Optical soliton interaction with $\kappa = 1$, $\tau = 0.5$ and $\kappa = 1$, $\tau = 0.25$.

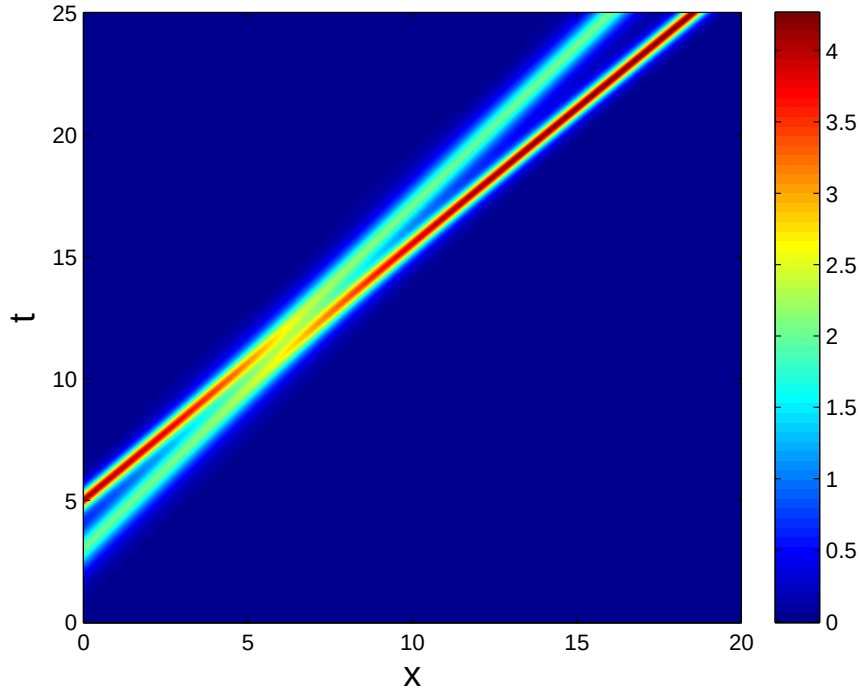

Another behavior unique to the soliton is elastic interaction. When two solitons interact, they emerge with shapes identical to those before interaction but with a phase shift. The computational result is illustrated in Figure 6. The same pulse as before is inserted into the medium with a more intense pulse following closely. A phase shift in both pulses is evident, but they propagate as expected.

The next step is to investigate more closely how solitons interact between energy levels. For example, counter-propagating pulses should experience a Doppler shift upon interaction. The magnitude of this phenomenon is limited by the approximations made for the slowly varying envelopes, but preliminary results indicate that it may still be observed.

4.2 Superflourescence

Another interesting optical phenomenon is superflourescence. This is the spontaneous emission of photons by many atoms, which creates a coherent pulse propagating through the medium. To set up the computational experiment, we must create an initial condition in which all atoms are in the first excited state. A small pulse is then injected into the medium. This perturbs the polarization and causes electrons to fall to the ground state, which in turn emits a field. The pulse continues to grow and the its interaction with the medium causes a

pattern to form in which large oscillations propagate forward and small oscillations propagate backward. The computational result is illustrated in Figure 7.

Figure 7: Superflourescence in a two-level medium.

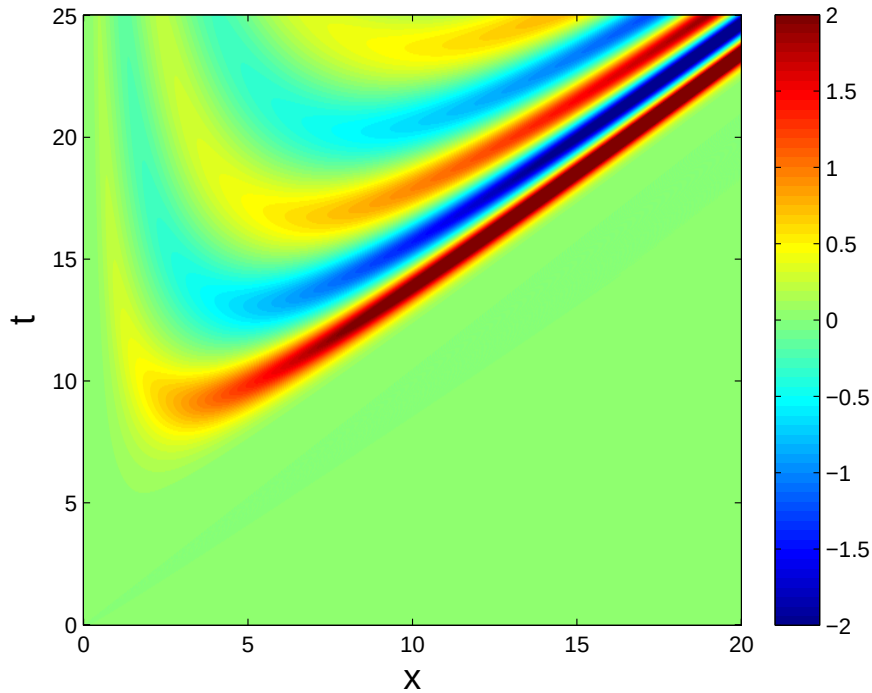

This phenomenon is analytically interesting because the solution is self-similar under a change of coordinates. In fact, it is closely related to a Bessel function. Additional details may be found in [1]. In the three-level system, it is possible to begin with all atoms in the second excited state. A small pulse corresponding to the upper transition frequency causes a this same phenomenon to occur when electrons fall to the first excited state. A secondary pulse is created when electrons fall to the ground state. Performing an analysis of the self-similar solution results in a dispersion relation with branch cut instabilities. This work is still preliminary, so the consequences are currently unknown. We hope to investigate further when time permits.

References

[1] L. Allen and J.H. Eberly. *Optical Resonance and Two-Level Atoms*. Dover Publications, 1987.

[2] A.I. Maimistov and A.M. Basharov. *Nonlinear Optical Waves*. Springer, 1999.

[3] Jerome V. Moloney and Alan C. Newell. *Nonlinear Optics*. Westview Press, 2004.